Measurement of the Heat Load Imposed on the Reactor Vessel Depending on the Crust Layer in a Severe Accident

2021. 05. 13

Joon-Soo Park, Hae-Kyun Park and Bum-Jin Chung *

Presenter: Joon-Soo Park

Kyung Hee University

Introduction (1/3)

- **IVR-ERVC (In-Vessel Retention – External Reactor Vessel Cooling)**

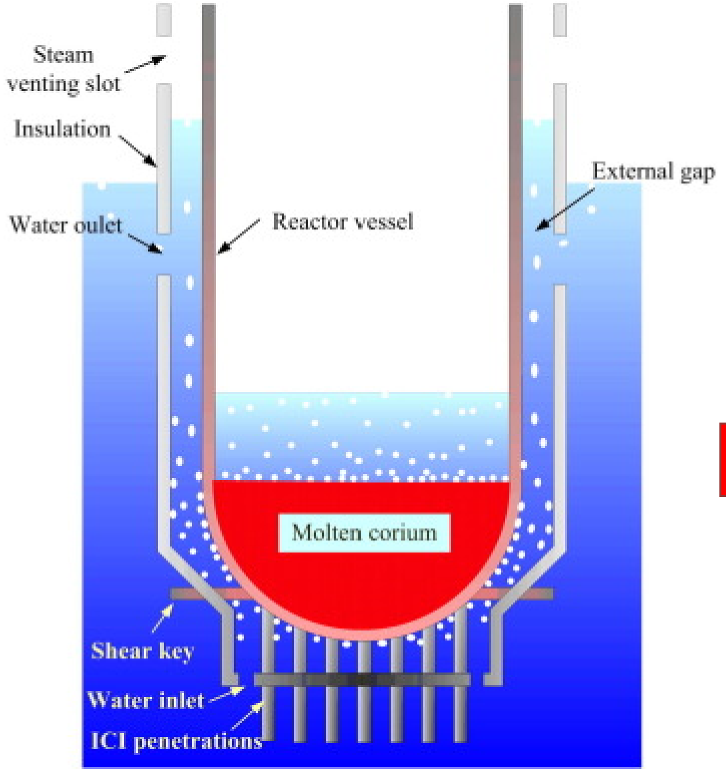

Schematic of IVR-ERVC

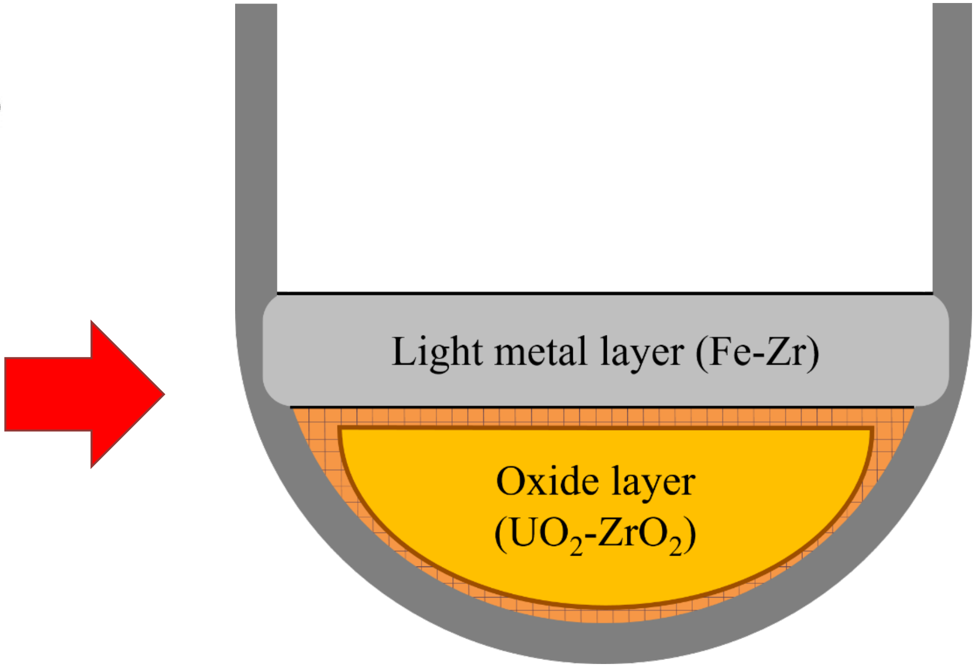

2-Layer Molten Pool Configuration

Introduction (2/3)

- **Flow Patterns**

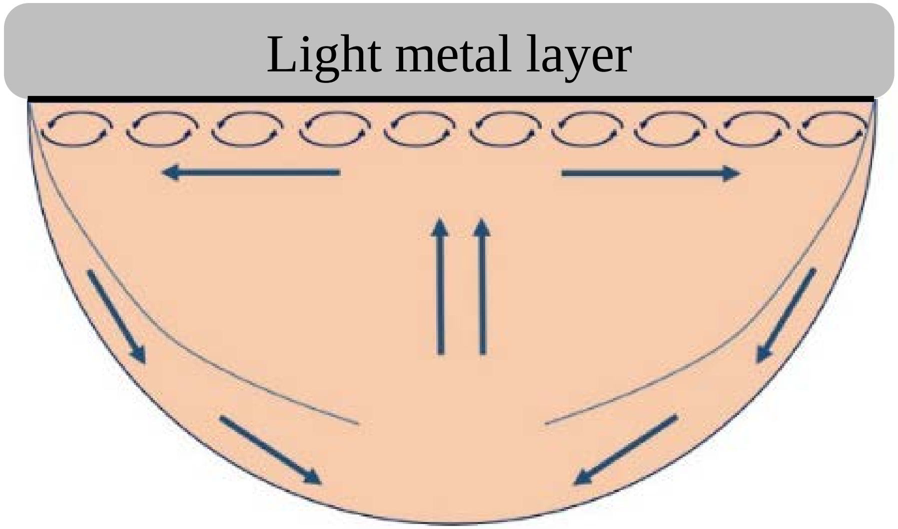

Flow Pattern at the 2-Layer Molten Pool [2]

- **Main flow:** The downward flows run down along the curved.
Then, the flow rises and move along upper region.

- **Upper convective flow:** Convective flow underneath the light metal layer.

Introduction (3/3)

- In response to the Fukushima accident, the IAEA introduced the DECs (Design Extension Condition) to prevent and mitigate such accidents and required detailed analysis for probable accident scenarios.
- Crust layer formation along the oxide layer boundary is one such scenario.
- The formation of crust layer changes the geometric and thermal boundary conditions of the oxide layer, affects natural convection heat transfer in the oxide layer.
- Few experimental studies were performed for crust layer effect.

Object of study

1. Heat flux distribution of oxide layer according to crust layer

2. To investigate separate effect of crust layer

→ Geometrical influence

→ Effect of thermal boundary condition

3. Simulation of oxide layer with crust using mass transfer experiments

Experimental methodology

- Analogy between heat transfer and mass transfer

Interests

Heat Transfer Problem → Mass Transfer Problem

Analogy concept ↓

Heat Transfer Solution ← Mass Transfer Solution

[Governing equations]

Heat transfer	Mass transfer
$\frac{\partial u}{\partial x}+\frac{\partial u}{\partial y}=0$	
$\rho\frac{Du}{Dt}=-\frac{\partial P}{\partial x}+\mu\left(\frac{\partial^2 u}{\partial x^2}+\frac{\partial^2 u}{\partial y^2}\right)+X$	
$\frac{DT}{Dt}=\alpha\nabla^2 T$	$\frac{DC}{Dt}=D_m\nabla^2 C$

[Dimensionless numbers]

Heat transfer		Mass transfer	
Nu	$\frac{hH}{k}$	Sh	$\frac{h_m H}{D_m}$
Pr	$\frac{\nu}{\alpha}$	Sc	$\frac{\nu}{D_m}$
Ra	$\frac{g\beta\Delta T H^3}{\alpha\nu}$	Ra	$\frac{gH^3}{D_m\nu}\frac{\Delta\rho}{\rho}$

Copper electroplating system

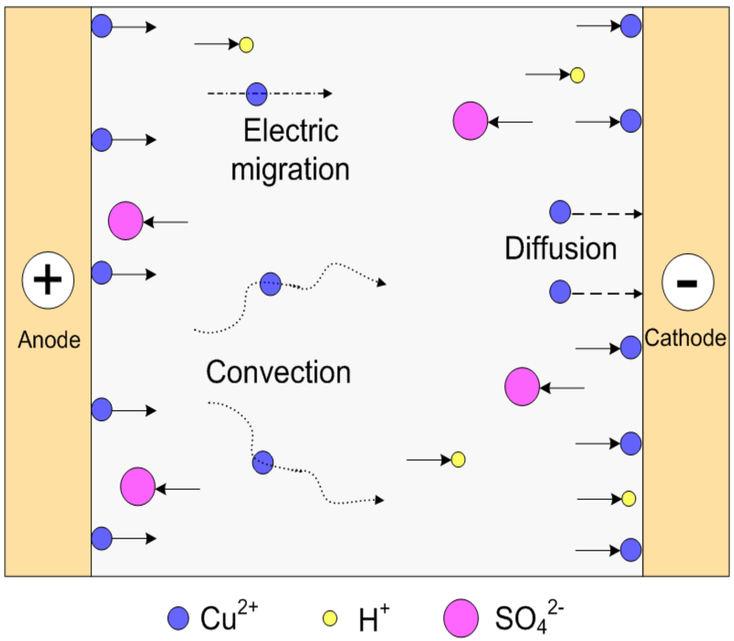

Anode : $Cu \rightarrow Cu^{2+} + 2e^{-}$

Cathode : $Cu^{2+} + 2e^{-} \rightarrow Cu$

- **Total mass transfer rate (N_t)**

  = Diffusion (N_d) + Convection (N_c) + Electric migration (N_m)

  Not exist in heat transfer, thus suppress it using H_2SO_4

- **Mass transfer coefficient**

$$h_m = \frac{(1-t_n) I_{lim}}{nF(C_b - C_s)}$$

  I_{lim} → Measurement

  C_s → $C_s \approx 0$

$$h = \frac{q''}{(T_h - T_c)}$$

- **Advantage of mass transfer**
  - To achieve high Rayleigh number for small facility
  - No heat leakage
  - No radiation heat transfer

Modified Rayleigh number in mass transfer

[Heat transfer]		**[Mass transfer]**
$Da = \dfrac{q'''H^2}{k\Delta T}$	→	$Da_m = \dfrac{(1-t_{Cu^{2+}})I'''H^2}{nFD_m\Delta C}$
$Ra'_H = \dfrac{g\beta q'''H^5}{\alpha\nu k}$	→	$Ra'_H = \dfrac{(1-t_{Cu^{2+}})gI'''H^5\Delta\rho}{nFD_m{}^2\mu\Delta C}$

q''' (Volumetric heat generation)	I''' (Volumetric current)
T (Temperature)	C (Concentration)
k (Thermal conductivity)	D_m (Mass diffusivity)

Oxide layer modeling

- **Applied assumptions for oxide layer modeling**

1. The outer vessel wall is maintained under isothermal conditions.

2. The temperature difference between inner and outer vessel wall is neglected.

3. The temperature of the crust is the same as the melting temperature of the oxide layer.

Crust modeling (1/5)

- **Determiantion of crust thickness**

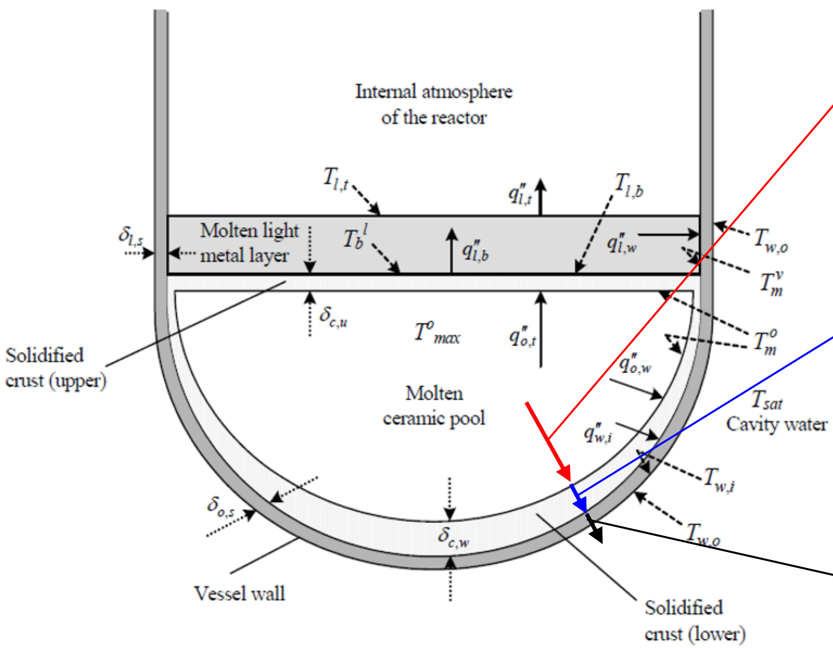

Schematic of the 2-Layer Molten Pool [3]

Convective HT

$$q''_{o,w} = h_{o,w}(T^o_{max} - T^o_m) = \frac{k_{crust}}{\delta_{crust}}(T^o_{max} - T^o_m) - \frac{Q'''_{crust}\delta_{crust}}{2} \quad (1)$$

Conductive HT

$$q''_{w,i} = \frac{k_{crust}}{\delta_{crust}}(T^o_m - T_{w,i}) + \frac{Q'''_{crust}\delta_{crust}}{2} = \frac{k_{wall}}{\delta_{wall}}(T_{w,i} - T_{w,o}) \quad (2)$$

Boiling HT

$$q''_{w,o} = q''_{w,i} = C_{boil}(T_{w,o} - T_{sat})^3 \quad (3)$$

Crust modeling (2/5)

- **Comparison calculation results with ERI code**

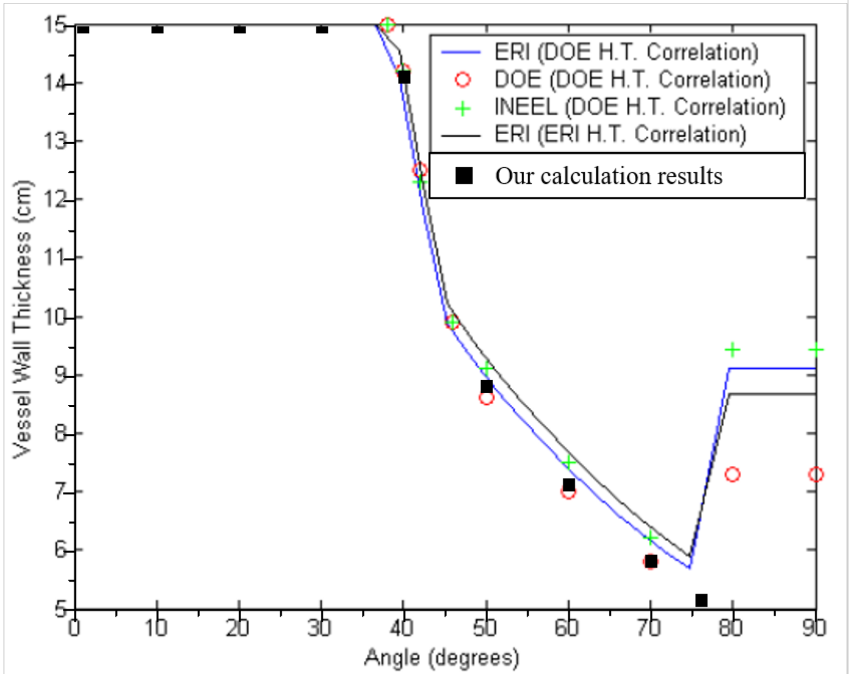

(a) Vessel wall thickness

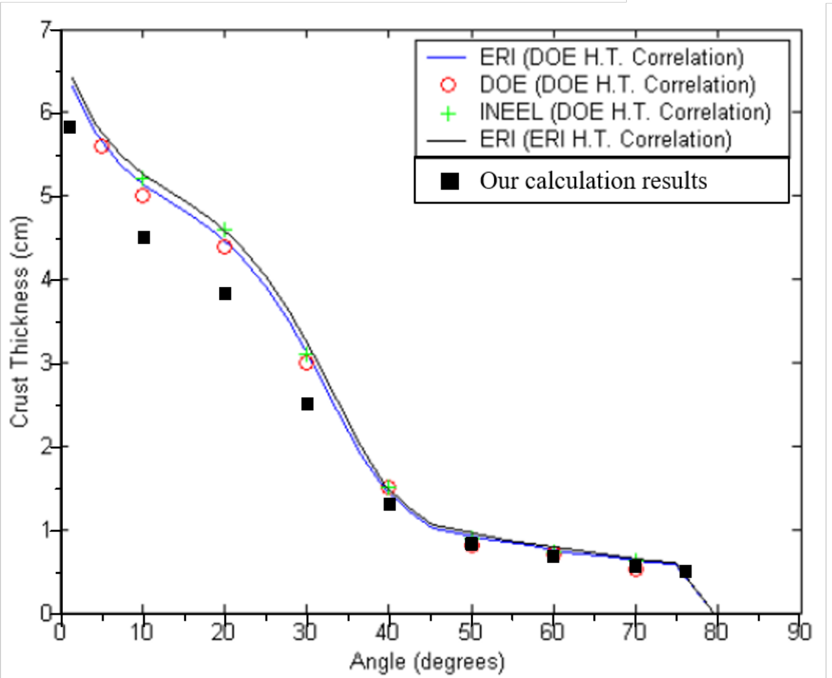

(b) Crust thickness

→ Our calculation results for AP1000 well agreed with ERI code results.

Crust modeling (3/5)

- **Crust thickness at each decay heat**

Decay heat (W)	Crust thickness (m)	
	Prototype	Scale down
10^6	0.17	0.007
10^3	1.06	0.042

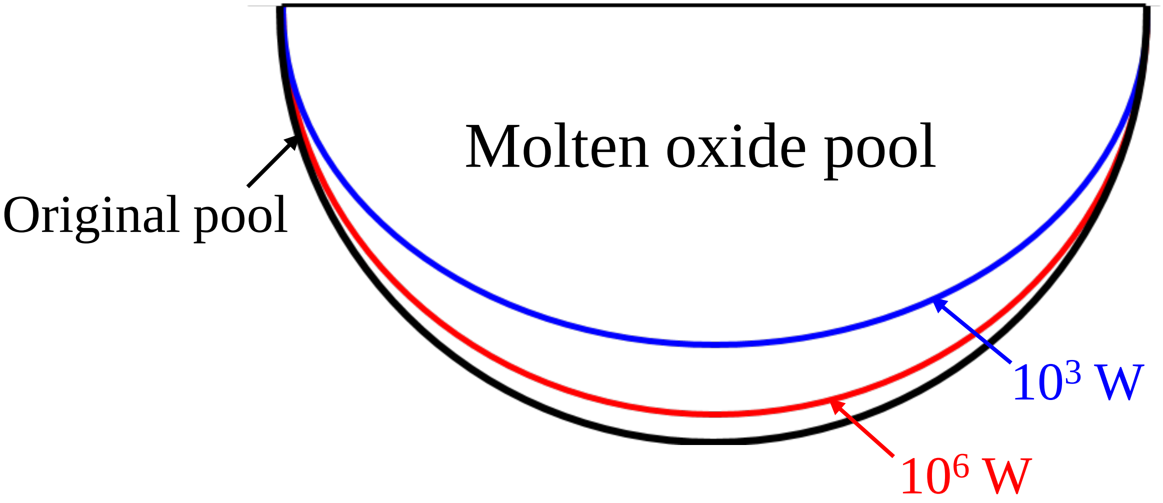

Crust modeling (4/5)

- **Thermal boundary condition**

<table>
<tr><th colspan="3">$Ra'_H = Ra_H \times Da$</th></tr>
<tr><td></td><td>w/o Crust</td><td>w/ Crust</td></tr>
<tr><td>Heat Transfer</td><td>

$$\frac{g\beta q''' H^5}{\alpha\nu k} = \frac{g\beta \Delta T_1 H^3}{\alpha\nu} \times \frac{q''' H^2}{k\Delta T_1}$$

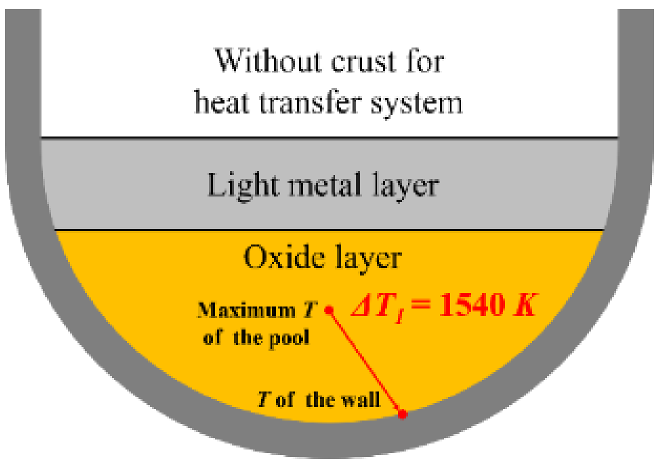

</td><td>

$$\frac{g\beta q''' H^5}{\alpha\nu k} = \frac{g\beta \Delta T_2 H^3}{\alpha\nu} \times \frac{q''' H^2}{k\Delta T_2}$$

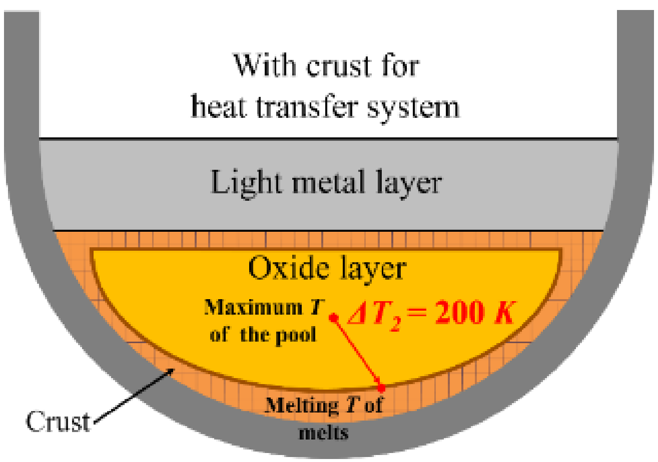

</td></tr>
</table>

Crust modeling (5/5)

- **Thermal boundary condition**

$Ra'_H = Ra_H \times Da$		
	w/o Crust	w/ Crust
Mass Transfer	$\frac{(1-t_{Cu^{2+}})I'''gH^5\Delta\rho}{nFD_m^2\mu\Delta C} = \frac{gH^3\Delta\rho}{D_m\mu} \times \frac{(1-t_{Cu^{2+}})I'''H^2}{nFD_m\Delta C}$ 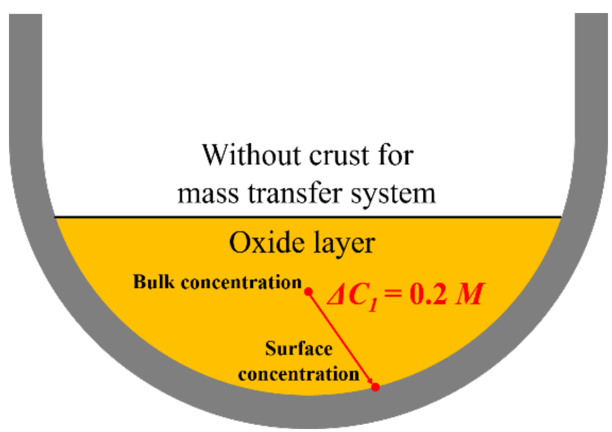	$\frac{(1-t_{Cu^{2+}})gI'''H^5\Delta\rho}{nFD_m^2\mu\Delta C} = \frac{gH^3\Delta\rho \times \frac{\Delta T_2}{\Delta T_1}}{D_m\mu} \times \frac{(1-t_{Cu^{2+}})I'''H^2}{nFD_m\Delta C \times \frac{\Delta T_2}{\Delta T_1}}$ 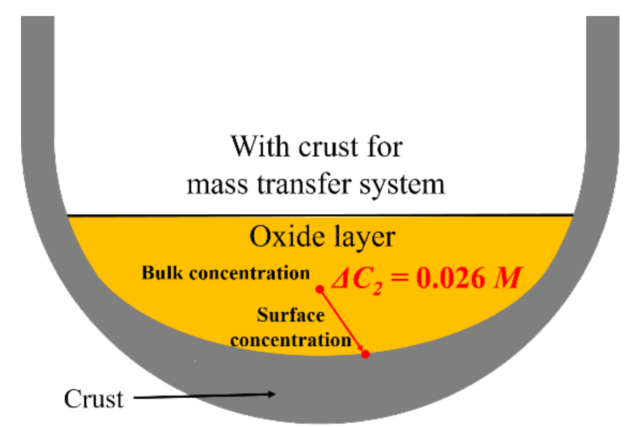

Test matrix

Crust Formation	Crust Thickness (m)	Ra'_H	Boundary Condition		Pr
			Curved Surface	Uppermost Region	
w/o Crust	0	9.51×10^{14}	Isothermal	Isothermal	2283
w/ Crust	0.003	6.23×10^{13}			1979
	0.01	4.79×10^{13}			
	0.03	1.61×10^{13}			
	0.05	3.97×10^{12}			

Test Rigs

- **MassTER-OP2(CL)**

  : Mass Transfer Experimental Rig for 2D Oxide Pool with Crust layer

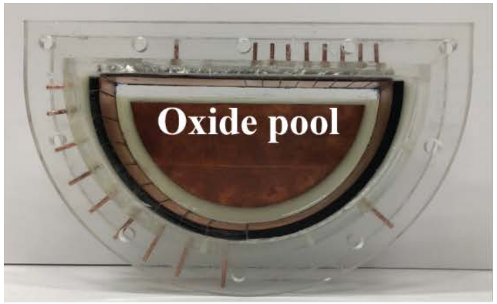

(a) Without crust

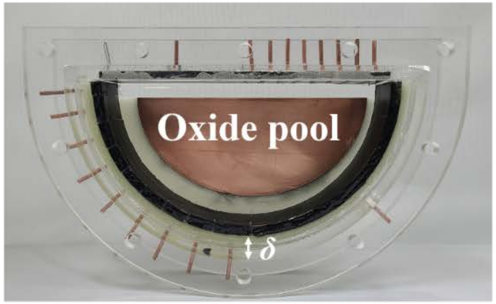

(b) Crust: 0.003 m

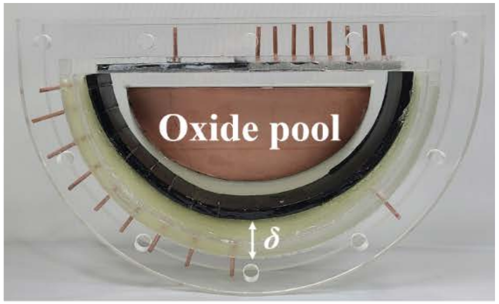

(c) Crust: 0.01 m

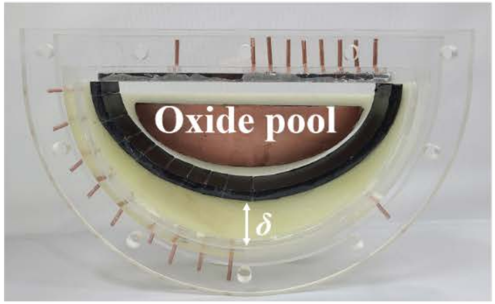

(d) Crust: 0.03 m

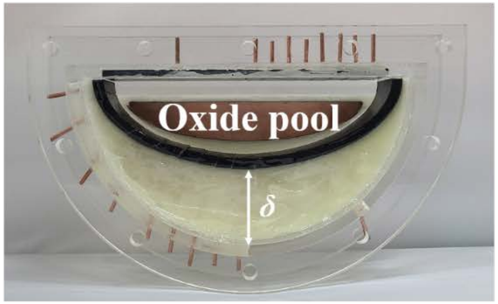

(e) Crust: 0.05 m

- Radius = 0.1 m, Width = 0.04 m

Test circuit

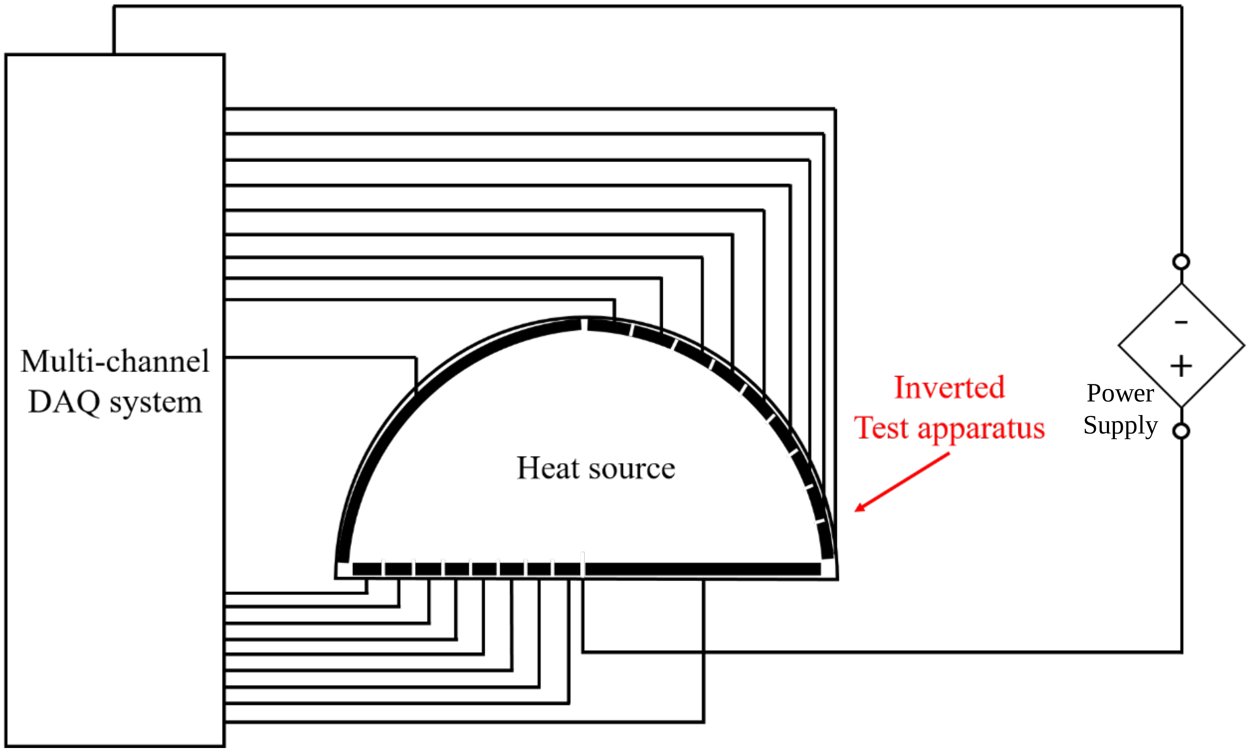

Comparison with existing studies

- **Comparison of the measured *Nu* with existing studies**

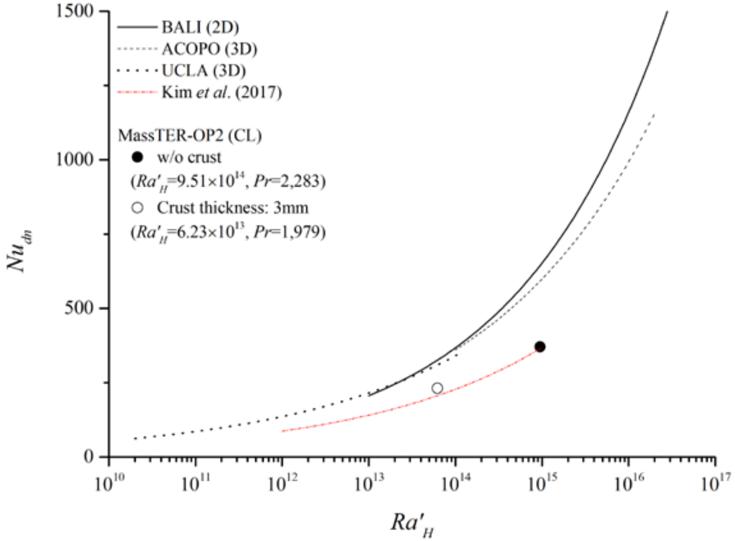

(a) Mean Nu_{dn} of the curved surface

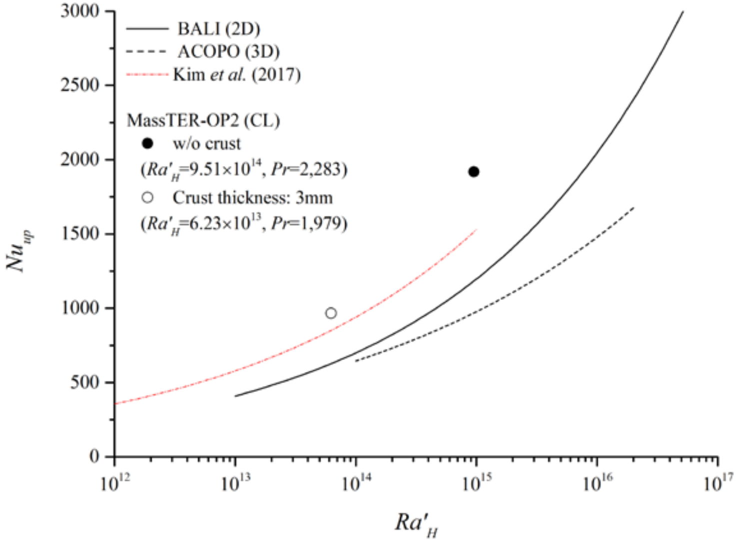

(b) Mean Nu_{dn} of the uppermost region

→ The discrepancies are associated with the high *Pr* of our mass transfer system.

→ Nu_{mean} values are 16% (for crust free) and 18% (for 3 mm thick crust) higher than the BALI correlation.

→ The overall trend between Ra'_H and *Nu* was similar.

Effect of the crust layer

- **Local heat transfer according to thermal boundary condition**

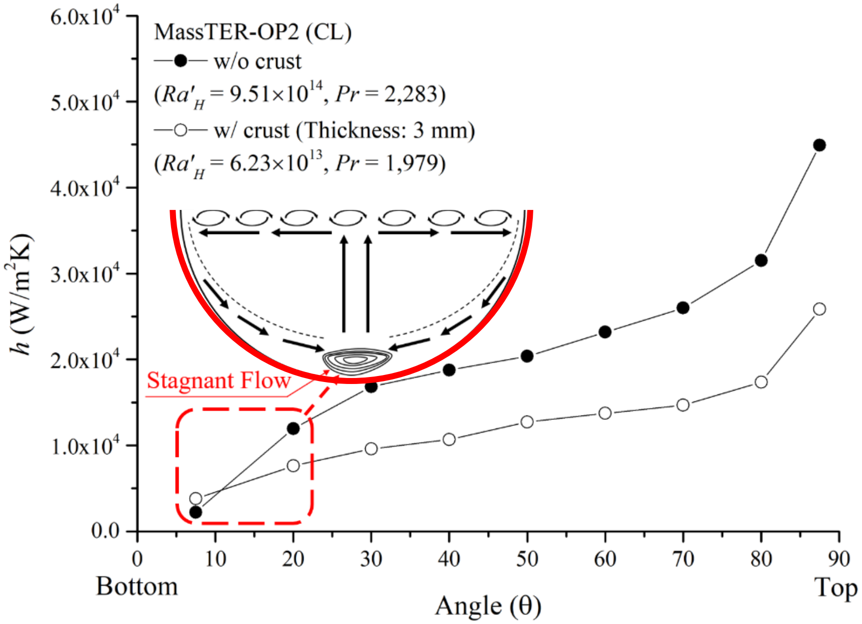

(a) h_{loc} of the curved surface

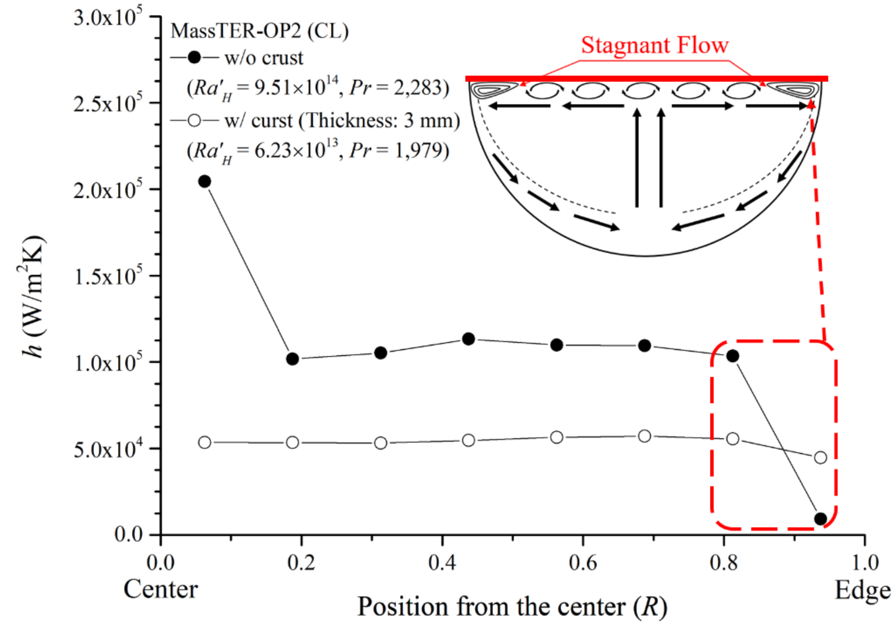

(b) h_{loc} of the uppermost region

→ Heat transfer decreased with crust layer acting as a thermal resistance.

→ Stagnant flows formed regardless of the crust layer.

Influence of crust thickness

- **Local heat transfer according to crust thickness**

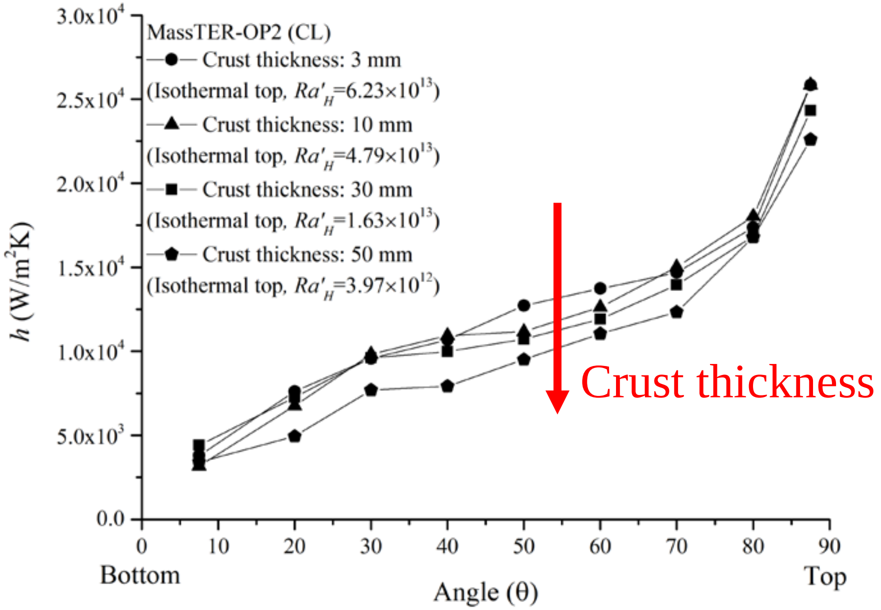

(a) h_{loc} of the curved surface

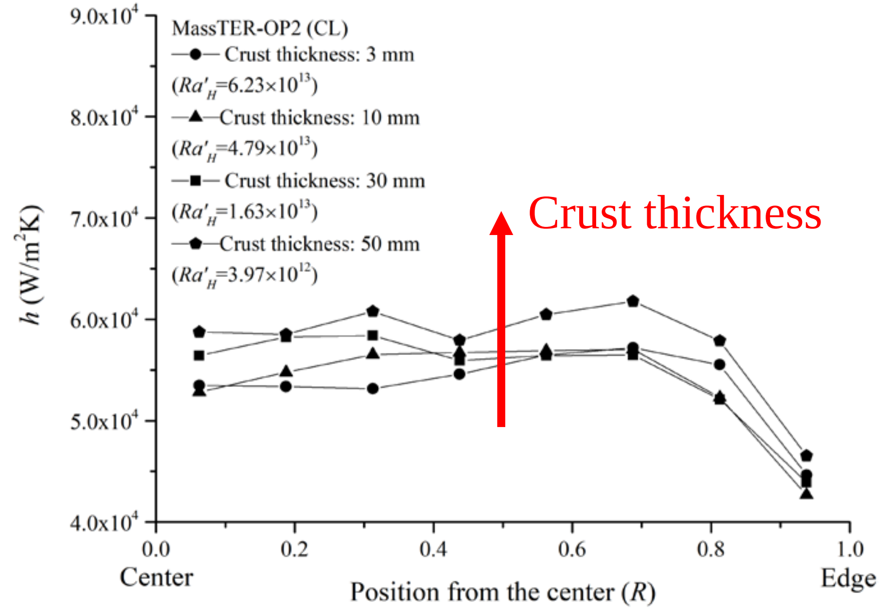

(b) h_{loc} of the uppermost region

→ Heat transfer at the curved surface decreased as the crust layer became thicker.

→ Heat trasnfer at the uppermost of oxide layer increased with crusth thickness.

Conclusions

- Natural convection heat transfer of the oxide layer with crust was simulated by mass transfer experiments.

  → Modeling of crust layer was performed to setup the crust geometries and the thermal boundary conditions.

- Effect of thermal boundary condition: Heat transfer ↓, Crust acts as a thermal resistance.

- Influence of crust thickness: Cooling length of oxide layer ↓

  - Curved surface: Driving force ↓, Heat transfer ↓

  - Uppermost region: ΔT between the rising plume and uppermost region ↑, Heat transfer ↑

- The influence of the crust layer varying the thermal boundary conditions was much larger than influence of varying the crust thickness.

Thank you for your attention !

References

[1] R.J. Park, K.S. Ha, H.Y. Kim, Detailed evaluation of natural circulation mass flow rate in the annular gap between the outer reactor vessel wall and insulation under IVR-ERVC, Annals of Nuclear Energy, Vol. 89, pp. 50—55, 2016.

[2] S.H. Kim, B.J. Chung, Mass transfer experiments on the natural convection heat transfer of the oxide pool in a three-layer configuration, Progress in Nuclear Energy, Vol. 106, pp. 11—19, 2018.

[3] H. Esmaili, M.K. Rahbar, Analysis of in-vessel retention and ex-vessel fuel coolant interaction for AP1000, U.S. NRC, 2004, NUREG/CR-6849, ERI/NRC-04-201.

Appendix (1/2)

[Heat transfer]

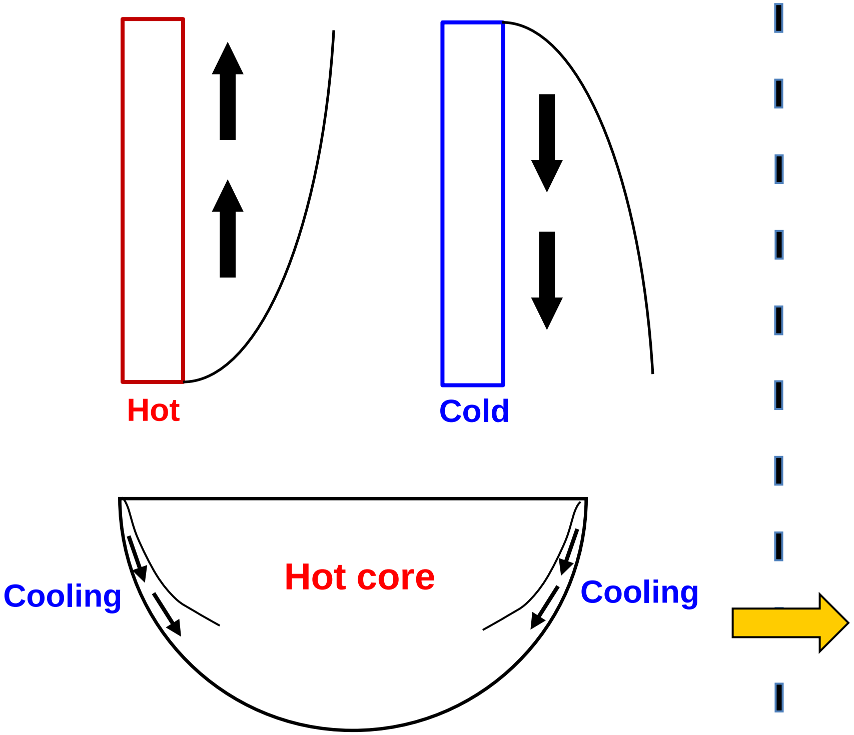

[Mass transfer]

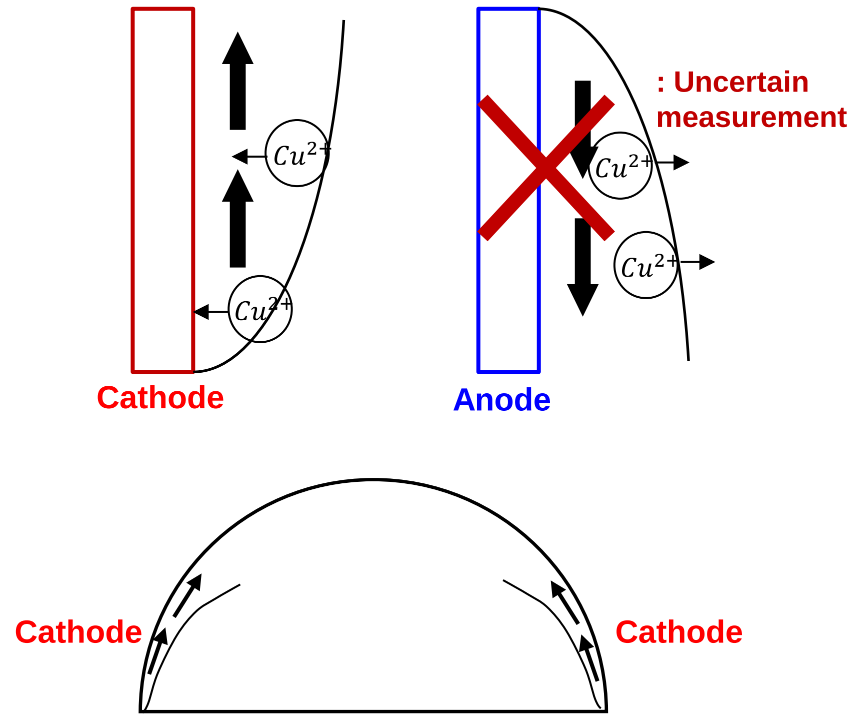

→ Inverted against gravity direction

Appendix (2/2)

- **Comparison of flow patterns depending on *Pr* in oxide layer**

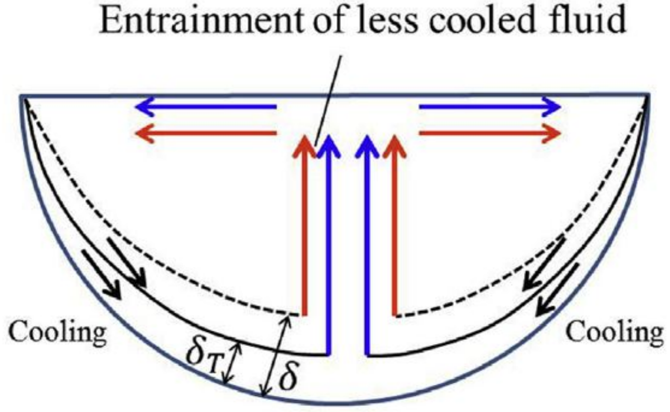

$Pr > 1$

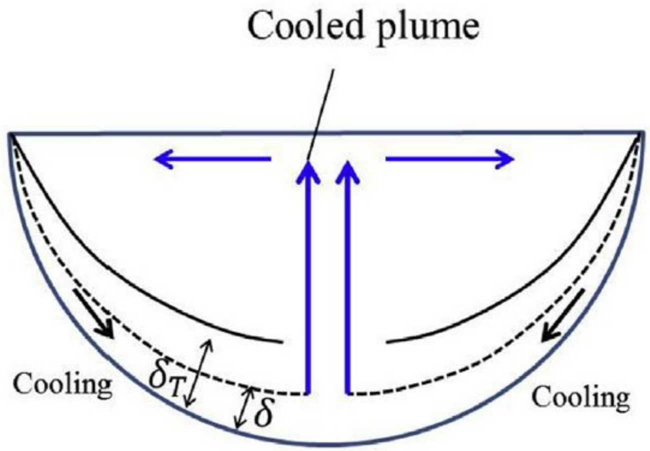

$Pr < 1$

→ The momentum boundary layer is thicker than thermal boundary layer.

→ Thus, the less cooled fluid was entrained to the rising plume.

→ This is the reason for the discrepancies between our experimental results and existing studies.